Validation of Aura Microwave Limb Sounder Ozone by Ozonesonde and Lidar Measurements

Y.B. Jiang[1], L. Froidevaux[1], A. Lambert[1], N.J. Livesey[1], W.G. Read[1], J.W. Waters[1], B. Bojkov[2], T. Leblanc[3], I.S. McDermid[3], S. Godin-Beekmann[4], M.J. Filipiak[5], R.S. Harwood[5], R.A. Fuller[1], W.H. Daffer[1], B.J. Drouin[1], R.E. Cofield[1], D.T. Cuddy[1], R.F. Jarnot[1], B.W. Knosp[1], V.S. Perun[1], M.J. Schwartz[1], W.V. Snyder[1], P.C. Stek[1], R.P. Thurstans[1], P.A. Wagner[1], M. Allaart[6], S.B. Andersen[7], G. Bodeker[8], B. Calpini[9], H. Claude[10], G. Coetzee[11], J. Davies[12], H. De Backer[13], H. Dier[14], M. Fujiwara[15], B. Johnson[16], H. Kelder[17], N. P. Leme[18], G. König-Langlo[19], E. Kyro[20], G. Laneve[21], L. S. Fook[22], J. Merrill[23], G. Morris[24], M. Newchurch[25], S. Oltmans[26], M.C. Parrondos[27], F. Posny[28], F. Schmidlin[29], P. Skrivankova[30], R. Stubi[31], D. Tarasick[32], A. Thompson[33], V. Thouret[34], P. Viatte[35], H. Vömel[36], P. von Der Gathen[37], M. Yela[38], G. Zablocki[39]

[1]Jet Propulsion Laboratory, California Institute of Technology, Pasadena, CA, USA
[2] NASA Goddard Space Flight Center, Greenbelt, MD, USA
[3]Jet Propulsion Laboratory, California Institute of Technology, Table Mountain Facility, Wrightwood, CA, USA
[4] Service d'Aeronomie/IPSL, CNRS-Universite Pierre et Marie Curie, Paris, France
[5]Institute of Atmospheric and Environmental Science, University of Edinburgh, Edinburgh EH9 3JZ, Scotland, UK
[6]Royal Netherlands Meteorological Institute (KNMI), de Bilt, Netherlands
[7]Danish Meteorological Institute (DMI), Copenhagen, Danemark
[8]National Institute of Water and Atmospheric Research (NIWA), Lauder, Central Otago, New Zeland
[9]MeteoSwiss, Aerological Station Payerne, Payerne, Switzerland
[10]German Weather Service (DWD), Meteorological Observatory Hohenpeissenberg, Hohenpeissenberg, Germany
[11]South African Weather Service (SAWS), Irene, South Africa
[12]Environment Canada (EC), Downsview, ON, Canada
[13]Royal Meteorological Institute of Belgium (R.M.I.B.), Belgium
[14]German Weather Service (DWD), Meteorological Observatory Lindenberg, Lindenberg, Germany
[15]Graduate School of Environmental Earth Science, Hokkaido University, Sapporo, Japan
[16]NOAA/ESRL, Global Monitoring Division, Boulder, CO, USA
[17]Royal Netherlands Meteorological Institute (KNMI), de Bilt, Netherlands
[18]Instituto Nacional de Pesquisas Espaciais (INPE), Laboratorio De Ozonio, Sao Paulo, Brazil
[19]Alfred Wegener Institute for Polar and Marine Research (AWI), Bremerhaven, Germany
[20]Finnish Meteorological Institute (FMI), Arctic Research Center, Sodankyla, Finland
[21]U. Rome "La Sapienza", Rome, Italy
[22]Malaysian Meteorologial Service (MMS), Jalan Sultan, 46667 Petaling Jaya;Selangor Malaysia
[23]University of Rhode Island, Graduate School of Oceanography, Narragansett, RI, USA

[24]Valparaiso University, Valparaiso, IN, USA
[25]University of Alabama-Huntsville, Atmospheric Science Department, Huntsville, AL, USA
[26]NOAA/ESRL, Global Monitoring Division, Boulder, CO, USA
[27]National Institute for Aerospace Technology (INTA), Madrid, Spain
[28]Laboratoire de l'Atmosphere et des Cyclones (LACy), La Reunion, France
[29]NASA Goddard Spcace Flight Center, Wallops Island, VA, USA
[30]Czech Hydrometeorological Institute (CHMI), Prague, Czech Republic
[31]MeteoSwiss, Aerological Station Payerne, Payerne, Switzerland
[32]Environment Canada (EC), Downsview, ON, Canada
[33]Pennsylvania State University (PSU), State College, PA, USA
[34]Laboratoire d'Aerologie du CNRS (CNRS/LA), Toulouse, France
[35]MeteoSwiss, Aerological Station Payerne, Payerne, Switzerland
[36]Cooperative Institute for Research in Environmental Science, University of Colorado, Boulder, CO, USA
[37]Alfred Wegener Institute (AWI), Potsdam, Germany
[38]National Institute for Aerospace Technology (INTA), Madrid, Spain
[39]Institute of Meteorology and Water Management (IMGW), Legionowo, Poland

Abstract

We present validation studies of MLS version 2.2 upper tropospheric and stratospheric ozone profiles using ozonesonde and lidar data. Ozone measurements from over 60 ozonesonde stations worldwide and three lidar stations are compared with coincident MLS data. The MLS ozone stratospheric data between 150 and 3 hPa agree well with ozonesonde measurements; within 7% for the global average. Comparisons between MLS and ground-based lidar measurements from Hawaii, from the Table Mountain Facility, CA, and from the Observatoire de Haute-Provence (OHP), France, give very good agreement, within ~5%, for the stratospheric values. MLS values at 215 hPa are biased high compared to ozonesondes by ~20% at mid- to high latitude, although there is a lot of variability in this altitude region. The comparisons between MLS and the Table Mountain Facility tropospheric ozone lidar show ~8% agreement from 100 to 215 hPa, better than that indicated by the ozonesonde data. Continued MLS validation efforts for the 215 hPa pressure level are desirable. We obtain good global average agreement

between MLS and ozonesonde partial column values down to 215 hPa, although the MLS values at low- to mid latitudes are higher than the ozonesonde values by up to a few percent. MLS v2.2 ozone data agree better than the MLS v1.5 data with ozonesonde and lidar measurements. MLS tropical data show the wave one longitudinal pattern in the upper troposphere, with similarities to the average distribution from ozonesondes. High upper tropospheric ozone values are also observed by MLS in the tropical Pacific from June to November.

1. Introduction

Tropospheric pollution and the global effects of regional pollution have received increased attention in the past decade. Tropospheric ozone is a precursor of OH radicals and as such influences tropospheric chemistry and global climate change. Ozone distribution in the upper troposphere and lower stratosphere (UT/LS) is the result of a combination of transport and chemical processes. The zonal wave one in the tropical distribution of ozone and the tropical Atlantic ozone paradox [*Thompson et al.*, 2003] are interesting examples of variations in tropospheric ozone, and better characterization of the spatial and temporal variations of tropospheric ozone is needed. Ground-based observations of ozone are generally accurate, but relatively sparse globally.

The Microwave Limb Sounder (MLS) is one of four instruments on the Earth Observing System (EOS) Aura satellite which was launched on July 15, 2004 and placed into a near-polar orbit at ~705 km altitude, with a ~1:45 p.m. ascending equatorial crossing time. The Aura mission objectives are to study the Earth's ozone, air quality, and climate [*Schoeberl et al.*, 2006a, b]. MLS [*Waters et al.*, 1999, 2006] contributes to this objective by measuring atmospheric temperature profiles from the troposphere to the

thermosphere, and more than a dozen atmospheric constituent profiles, as well as cloud ice water content [*Wu et al.*, 2006] from millimeter- and submillimeter-wavelength thermal emission of Earth's limb with seven radiometers covering five broad spectral regions.

Initial ozone validation results using MLS v1.5 data include the early work of *Froidevaux et al.* [2006], as well as results of comparisons between MLS and ground-based microwave profiles [*Hocke et al.*, 2006], and the analyses of *Ziemke et al.* [2006] and *Yang et al.* [2007], focusing on stratospheric columns and resulting tropospheric ozone residual column abundances, using a combination of MLS and OMI data.

In this paper, we present validation results of the newly released MLS version 2.2 (or v2.2) ozone product from the upper troposphere to the upper stratosphere through comparisons with global ozonesonde and ground-based lidar measurements. Although MLS measures ozone in several spectral bands [*Waters et al.*, 1999, 2006], this paper focuses on the 'MLS standard product' for ozone, which is obtained from radiance measurements near 240 GHz and provides the best overall precision for the widest vertical range. There are related papers focusing on validation of the 240 GHz MLS ozone (and CO) data in the upper troposphere and lower stratosphere [*Livesey et al.*, 2007], mainly for pressures of 100 hPa and larger, and in the stratosphere and lower mesosphere [*Froidevaux et al.*, 2007], using satellite, aircraft and ground-based ozone measurements. Version 2.2 is currently in the early stages of reprocessing and is therefore more limited in terms of available days than version 1.5, with about 3 months of v2.2 reprocessed data, covering selected days in 2004, 2005, and 2006. A recent minor

software patch has led to version 2.21, with results that are essentially identical to v2.20 results for the vast majority of days.

In section 2, we summarize the data usage and screening recommendations for MLS v2.2 ozone profiles. Section 2 also provides a brief description of the estimated MLS ozone uncertainties, both random and systematic, which we generally refer to as precision and accuracy. We provide the comparisons between MLS ozone and ozonesonde profiles in section 3, followed by section 4 on ground-based lidar measurement comparisons. Section 5 summarizes the results and suggest improvements needed in future versions.

2. MLS Ozone Measurements

For an overview of the MLS spectral bands, main line frequencies, and target molecules, see *Waters et al.* [2006]. The overall MLS retrieval approach is discussed by *Livesey et al.* [2006] and the calculation specifics of the MLS radiance model (or 'forward model') are described by *Read et al.* [2006] and *Schwartz et al.* [2006]. MLS radiance spectra and residuals are discussed by *Livesey et al.* [2007] and *Froidevaux et al.* [2007], who show that the radiance fits are generally very good (within ~1%) although there is typically poorer closure in the lowermost height region (upper troposphere).

2.1 Data Usage and Screening

The MLS v2.2 ozone data files provide the ozone abundance fields as well as the estimated (single profile) precision fields and related data screening flags. A detailed illustration of these data screening fields is given by *Livesey et al.* [2005] for MLS v1.5 data. The recommendations for screening the MLS v2.2 ozone profiles are similar but not

identical to those given by *Livesey et al.* [2005] for version 1.5 data. We recommend the use of only even values of the "Status" field. Also there is now a slightly different threshold value for the "Quality" flag, which refers to the overall radiance fit for each profile; users should use only Quality > 0.4 for the stratosphere [*Froidevaux et al.*, 2007] and Quality > 1.2 for the upper troposphere [*Livesey et al.*, 2007]; we have conservatively used the latter value in this work. A new field named "Convergence" is also used in v2.2, and it refers to the ratio of the radiance fit chi square value for each profile to the chi square value that the retrieval would have been expected to reach. Users should retain only ozone profiles with Convergence < 1.8, which eliminates only about 1% of the available daily ozone profiles.

The data usage guidelines for MLS v2.2 ozone are summarized in Table 1. While more work of a very detailed nature is needed to further refine the data screening recommendations provided above, these recommendations will generally safely allow for the use of more than roughly 97% of the available daily MLS ozone profiles. As the retrievals at pressures larger than 215 hPa are not deemed satisfactory enough at this time [*Livesey et al.*, 2007], we will only consider ozone at pressures of 215 hPa or less in the following comparisons.

Table 1. MLS v2.2 Ozone Data Usage Guidelines.

Flag	Meaning/Usage	Values to use
Status	Can indicate operational or retrieval problems, and possible influence of clouds	Even
Quality	Radiance fit by the retrieval algorithms	>0.4 (stratosphere) >1.2 (upper troposphere)

Convergence (new for v2.2)	Ratio of the radiance fit to that expected by the retrieval algorithms	< 2.0
Precision	Negative if large contribution of a priori to the retrieved value	> 0
Pressure Range	Useful vertical range	215 hPa - 0.02 hPa

2.2 Resolution, Precision, and Accuracy

As described for atmospheric retrievals by Rodgers [1976], the vertical and horizontal (along the MLS sub-orbital track) resolutions can be visualized through the use of the averaging kernel matrix (Figure 1). The integrated value of the averaging kernels for ozone is generally very close to unity in the region from 215 to 0.01 hPa where the influence of a priori profile information on the retrievals is negligible. The vertical resolution is 2.7 to 3 km from the upper troposphere to the lower mesosphere.

The precision of the MLS ozone profiles is estimated by the MLS retrieval calculations, following the Rodgers [1976] formulation; these uncertainty estimates are provided in the MLS Level 2 files (for each profile), as the diagonal values of the error covariance matrix. The estimated root mean square precision for MLS ozone retrievals is typically fairly constant as a function of latitude; precision values can be as low as 20 to 30 ppbv from 100 to 215 hPa, and increase by an order of magnitude (~0.3 ppmv) near 1 hPa [*Froidevaux et al.*, 2007; *Livesey et al.*, 2007].

Simulation results for MLS ozone point to possible biases of about 5 to 10% (or 0.05 to 0.2 ppmv) for most of the stratosphere, down to 100 hPa, with precision (random errors on single profiles) of 2 to 30% [*Froidevaux et al.*, 2007]. Expected uncertainties increase, in percent, for MLS vertical retrieval grid pressures of 147 and 215 hPa,

especially in the tropics, where ozone abundances are low. The bias is the error one might expect to see in a multi-profile comparison versus 'true' profiles, whereas the total error is more relevant for single profile comparisons, as it includes a random component (scatter).

3. Comparisons of MLS and Ozonesonde Data

Ozonesondes are balloon-borne in situ instruments that continuously measure the ozone concentration as they ascend or descend in the atmosphere. A profile of ozone is obtained up to the burst point of the balloon – often at altitude in excess of 30 km or a pressure as low as 5 to 10 hPa. Ozonesonde measurements are the most accurate means of providing high vertical resolution ozone profiles. The detection limit is typically less than 2 ppbv, as compared to the typical clean background value of 30 ppbv for tropospheric ozone. Measurement uncertainty is about 10% in the troposphere, 5% in the stratosphere up to 10 hPa and 5-25% between 10 and 3 hPa [*Bodeker et al.*, 1998; *World Climate Research Programme*, 1998; *Smit et al*., 2007; *Kerr et al*, 1994; T*hompson et al.*, 2007]. We have used ozonesonde measurements available from the Aura Validation Data Center (AVDC) as well as some soundings from the World Ozone and Ultraviolet Data Center (WOUDC) in Toronto (http://www.woudc.org/). More than 70 stations were considered in this study, but considering the criteria we use to select the MLS and correlative data profiles and the availability of v2.2 and sonde data at the time of writing, some of the potentially available comparisons are currently missing. Figure 2 shows the global distribution of these stations. There is good coverage in the northern hemisphere high latitude, but the southern hemisphere coverage is sparse: only 4 stations at high

southern latitudes, and 1 (Lauder, New Zealand) at the southern mid-latitudes. The tropical stations are mainly from the Southern Hemisphere Additional Ozonesondes (SHADOZ) project. The ozonesonde sites and number of coincident profiles with MLS observations (when more than one exists) are listed in Table 2, with most of the data made available at the Aura Validation Data Center (AVDC); data from the sites labeled WOUDC were obtained directly from the WOUDC. Examination of ozonesonde measurements suggests that station-to-station biases exist between the different sites due to differences in data processing technique and sensor solution and varying hardware [*Johnson et al.*, 2002; *Thompson et al*., 2003; *Smit et al*., 2007].

Table 2. Ozonesonde site information for comparisons used in this work.

Site Name	Latitude	Longitude	Contact or data source	Number of coincident profiles with Aura MLS
Alert (NU), Canada	82.50	-62.33	D. Tarasick/J. Davies (EC/MSC)	10
Ascension Island, United Kingdom	-7.98	-14.42	F. Schmidlin (NASA/GSFC)	8
Belgrano (Argentina), Antarctica	-77.85	-34.55	M. Yela (INTA)	9
Boulder (CO), Canada	40.00	-105.25	S. Oltmans/B. Johnson (NOAA/ESRL)	16
Bratts.Lake (SK), Canada	50.20	-104.70	D. Tarasick/J. Davies (EC/MSC)	5
Churchill (MB), Canada	58.74	-94.07	D. Tarasick/J. Davies (EC/MSC)	5
Cotonou, Benin	6.21	2.23	A. Thompson (PSU), V. Thouret (CNRS/LA)	9
De.Bilt, Netherlands	52.10	5.18	M. Allaart (KNMI)	18
Edmonton (AB), Canada	53.55	-114.11	D. Tarasick/J. Davies (EC/MSC)	5
Egbert (ON), Canada	44.23	-79.78	D. Tarasick/J. Davies (EC/MSC)	5
Eureka (NU), Canada	79.99	-85.94	D. Tarasick/J. Davies (EC/MSC)	14
Goose.Bay (NF), Canada	53.31	-60.36	D. Tarasick/J. Davies (EC/MSC)	8

Heredia, Costa Rica	10.00	-84.10	H. Vömel (NOAA/ESRL)	4
Hilo (HI), USA	19.43	-155.04	S. Oltmans/B. Johnson (NOAA/ESRL)	6
Hohenpeissenberg, Germany	47.80	11.00	H. Claude (DWD)	50
Houston (TX), USA	29.72	-95.40	G. Morris (Valparaiso U.)	5
Huntsville (AL), USA	35.28	-86.59	S. Oltmans (NOAA/ESRL) M. Newchurch (U. Alabama-Huntsville)	14
Irene, South Africa	-25.90	28.22	A. Thompson (PSU), G. Coetzee (SAWS)	5
Jokioinen, Finland	60.80	23.50	E. Kyro (FMI)	9
Kagoshima, Japan	31.60	130.60	JMA, WOUDC	5
Keflavik, Iceland	63.97	-22.60	M. C. Parrondos (INTA)	14
Kelowna (BC), Canada	49.93	-119.40	D. Tarasick/J. Davies (EC/MSC)	5
La Reunion, France	-21.06	55.48	F. Posny (U. de La Reunion)	9
Lauder, New Zealand	-45.04	169.68	G. Bodeker (NIWA)	17
Legionowo, Poland	52.40	20.97	Grzegorz Zablocki (IMGW)	31
Lindenberg, Germany	52.20	14.10	Horst Dier (DWD)	17
Malindi, Kenya	-2.99	40.19	A. Thompson (PSU) G. Laneve (U. Rome)	2
Marambio (Argentina), Antarctica	-56.72	-64.23	E. Kyro (FMI)	16
Naha (Okinawa), Japan	26.20	127.70	JMA, WOUDC	11
Nairobi, Kenya	-1.27	36.80	B. Calpini (MeteoSwiss)	12
Narragansett (RI), USA	41.49	-71.42	S. Oltmans/B. Johnson (NOAA/ESRL) J. Merrill (U. Rhode Island)	10
Natal, Brazil	-5.42	-35.38	N. P. Leme (INPE) F. Schmidlin (NASA	7
Neumayer, Antactica	-70.70	-8.30	G. König-Langlo (AWI)	24
Ny Aalesund (Spitsbergen), Norway	78.93	11.95	P. von Der Gathen (AWI)	20
Pago Pago, American Samoa	-14.23	-170.56	S. Oltmans/B. Johnson (NOAA/ESRL)	12
Paramaribo, Surynam	5.81	-55.21	H. Kelder (KNMI)	22
Payerne, Switzerland	46.80	7.00	P. Viatte/R. Stubi (MeteoSwiss)	47
Praha, Czech Republic	50.00	14.45	P. Skrivankova (CHMI)	20
Resolute (NU), Canada	74.71	-94.97	D. Tarasick/J. Davies (EC/MSC)	2
San Cristobal (Galapagos),	-0.92	-89.60	S. Oltmans/B. Johnson (NOAA/ESRL)	5
Sapporo, Japan	43.10	141.30	JMA, WOUDC	15
Scoresbysund, Greenland	70.50	-22.00	S. B. Andersen (DMI)	13

Sepang (Kuala Lumpur), Malysia	2.73	101.70	A. Thompson (PSU), C.P. Leong (MMS)	3
Sodankyla, Finland	67.39	26.65	E. Kyro (FMI)	26
Summit, Greenland	72.60	-38.50	S. Oltmans/B. Johnson (NOAA/ESRL)	5
Suva, Fiji	-18.13	178.40	S. Oltmans/B. Johnson (NOAA/ESRL)	2
Syowa, Japan	-69.00	39.60	JMA, WOUDC	21
Tateno, Japan	36.10	140.10	JMA, WOUDC	13
Thule, Greenland	76.50	-68.70	S. B. Andersen (DMI)	7
Trinidad Head (CA), USA	40.80	-124.16	S. Oltmans/B. Johnson (NOAA/ESRL)	6
Uccle, Belgium	50.80	4.35	H..De Backer (KMI)	46
Wallops Island (VA), USA	37.90	-75.50	F. Schmidlin (NASA GSFC)	14
Watukosek (Java), Indonesia	-7.50	112.60	A. Thompson (PSU), M. Fujiwara (U. Hokkaido)	3
Yarmouth (NS), Canada	43.87	-66.11	D. Tarasick/J. Davies (EC/MSC)	5

In order to get good statistics, we choose the coincidence criteria for MLS and ozonesonde profiles to be within $\pm 2^{o}$ latitude, $\pm 10^{o}$ longitude and on the same (GMT) day. We have looked at the comparisons using tighter criteria and while the results yield some differences (not shown here), this will not affect the main conclusions given here. In the comparisons, we have filtered the MLS data as pointed out in Section 2.1, and used only cloud free profiles, based on the MLS cloud screening criteria (Status = 0). Figure 3 shows all the days available in 2004, 2005 and 2006 based on the coincidences between MLS v2.2 and ozonesonde profiles. We have degraded the high resolution ozonesonde profiles by using two methods: a least-squares fit of the fine resolution pressure grid to the MLS ozone retrieval grid, and also, the use of MLS averaging kernels (see Figure 1) to smooth the ozonesonde data after the least square fit to the MLS grid. The difference between these two methods is shown in Figure 4, where three representative profiles (northern high latitude, tropics, and southern high latitude) are shown. We see that there are negligible differences between the two methods, and the results of comparisons are

not very sensitive to the method chosen, as expected, due to the sharply peaked nature of the MLS averaging kernels. Nevertheless, we have degraded the ozonesonde high resolution profiles by using the averaging kernel method throughout this work.

As pointed out by *Froidevaux et al.* [2007], improved algorithms in MLS v2.2 ozone have generally led to reduced biases in comparison to MLS v1.5. For example, MLS v2.2 has largely corrected the small negative slope that existed in v1.5 comparisons with SAGE II. Figure 5 shows the average differences between ozonesonde profiles and MLS v2.2 and v1.5 data (for the same days) for six different latitude bins. MLS v2.2 data show better agreement with ozonesonde values than the MLS v1.5 data especially in the upper troposphere (215 – 100 hPa). MLS v2.2 profiles still show some high biases compared to ozonesondes in the lower altitude range, but there is agreement within ~30% in the 100 to 215 hPa range in each latitude bin. Atmospheric variability may explain some of the larger differences in the equatorial region at 100 hPa. The 316 hPa level is too noisy and unreliable, as indicated by the scatter plots in Figure 6, and we do not recommend the use of MLS ozone for this pressure level. The MLS data and ozonesonde data agree with each other in the stratosphere (50 hPa to 5 hPa) to within ~10%. In some latitude bins, the comparisons still show a small negative slope from the upper troposphere to about 10 hPa. The combined precision estimate (heavy solid line in Figure 5) is obtained from the root sum square (rss) of the (random) uncertainties provided in the MLS data files and the 5% precision assumed for ozonesonde measurements. The standard deviations of the differences (dashed line in Figure 5) are larger than these combined precision estimates, especially in the UT/LS, probably as a result of spatial or temporal atmospheric variability in both the MLS data and the ozonesonde

measurements. The peak of the standard deviations around 100 hPa in the southern hemisphere may indicate interesting ozone dynamics. The large percentage differences in the UT/LS may also be caused by the sensitivity of the retrieval in that region, since the ozone in that region only contributes a very small fraction of the total MLS ozone signal.

The MLS v2.2 ozone abundances are well correlated with the ozonesonde values at all pressure levels except at 316 hPa, as shown in Figure 6. The 316 hPa level ozone varies between -0.2 ppmv to 0.4 ppmv, and is not recommended for scientific use. The larger scatter for the upper tropospheric levels is consistent with the results shown in Figure 5. There are a few questionable profiles (outliers) at various levels. Figure 7 presents averaged difference (MLS minus ozonesonde) profiles for each station grouped by latitude bin. The largest percentage differences occur at 100 hPa in the equatorial region, and at 215 hPa for other latitude bins. Most of the averaged profiles (from each site) agree with MLS within 20% in the stratosphere and 50% in the upper troposphere.

Figure 8 summarizes the MLS and ozonesonde averaged comparisons for each site versus latitude, with abundances on the left side panel and percentage differences on the right panel. The MLS data track the ozonesonde data very well as a function of latitude. Both datasets show smaller ozone mixing ratios in the equatorial region and larger ozone at mid-to-high latitude from 215 hPa to 46 hPa, with a change in the sign of this latitudinal gradient from 21 to 10 hPa. This consistent picture points to the robustness of the MLS v2.2 retrievals even for the upper troposphere, where ozone contributes only a small fraction to the total emission. The small ozone mixing ratios (<100 ppbv) in the

equatorial region below 100 hPa level represent typical upper tropospheric ozone values, and will be examined in more detail in Figure 10.

In the upper troposphere and lower stratosphere (100 hPa to 215 hPa), the differences between MLS and ozonesondes are more than 20% for most of the stations in the region south of 40^{o}N, and differences tend to oscillate between positive and negative values. The differences are large at stations in the tropical region for all pressure levels. For each station within 46 hPa to 5 hPa, the MLS data and ozonesonde data agree with each other in the middle stratosphere (46 hPa ~ 5 hPa) to within 20% except for some stations in the tropics where the abundances are lower.

The well-known enhancements in tropospheric ozone over the tropical Atlantic [*Thompson et al.*, 2003; *Jourdain et al.*, 2007] are shown both in the MLS ozone data and in the ozonesonde measurements (Figure 9) in December, January, and February (DJF) and March, April, and May (MAM). This phenomenon appears to be associated with pollution from biomass burning in Africa and South America and the tropical circulation. Moreover, MLS data also show enhanced ozone in the tropical Pacific in June, July, and August (JJA), and in September, October, and November (SON), which may notappear in ozonesonde measurements because of their sparse coverage. The higher ozone in the tropical Pacific in JJA and SON may also be caused by biomass burning, followed by cross-continental transport of polluted air lofted into the upper troposphere. There is also the possibility that stratosphere-troposphere exchange plays a role. The lower stratosphere ozone in the tropical region is relatively uniform longitudinally and shows no signal of the tropospheric wave one pattern.

Figure 10 shows the comparisons in detail in the equatorial region at 215 hPa, 147 hPa and 100 hPa in the upper troposphere. The averaged differences for each station are within 30 ppbv at 215 hPa, 50 ppbv at 146 and 100 hPa, although there is significant variability from site to site. The standard errors are within about 30 ppbv, which is roughly consistent with the results of analyses by *Livesey et al.* [2007], using aircraft data sources. There is only marginal significance for the tropical upper tropospheric comparisons (see Figure 5), in terms of MLS biases versus the ozondesondes. The 215 hPa high bias of ~20% seen in that figure arises from the mid- and high latitudes.

Ozone column abundance is another parameter of interest used in the process of validating MLS data against ozonesonde measurements. The MLS column ozone abundances are estimated to have a (1 σ) precision of 3%, for a typical column value obtained from the integration of an individual MLS ozone profile [*Froidevaux et al*., 2007], with an estimated (2 σ) accuracy of 4% (or 8 DU). Comparisons of column ozone measurements from MLS and column data from the CCD based Actinic Flux Spectroradiometers (CAFS) during various Aura Validation Experiment (AVE) campaigns [*Petropavlovskikh et al*., 2007] confirm that such uncertainty estimates are reasonable, as do column comparisons between MLS and other satellite-based ozone measurements [*Yang et al*., 2007; *Froidevaux et al*., 2007]. Figure 11 gives the averaged ozone column from MLS v2.2 data and ozonesonde column from each station, and the differences. As expected from Figure 8, the ozone columns also show good correspondence in the meridional variations, and the mean differences are mostly within 10%. The typical standard error shown in the figure is about 15%. Therefore, there are no

significant biases between MLS and ozondesonde column (within the 95% confident level).

More detailed column ozone scatter plots of MLS versus ozonesonde column ozone above six selected pressure levels are shown in Figure 12; different latitude bins are color-coded in this plot. There is a 1.3% average difference (MLS values higher than sonde values) for columns above 316 hPa, and this difference decreases as pressure decreases. The correlation coefficients for all pressure levels are about 0.95; MLS column ozone in the tropics shows larger biases as expected from this plot.

4. Comparisons of MLS versus Lidar Ozone Data

We have analyzed comparisons between MLS ozone and ozone from four lidars located at three NDACC (Network for the Detection of Atmospheric Composition Change, formerly NDSC) stations [*Leblanc et al.,* 2000, *McDermid et al*., 1991; *Godin et al.*, 1989, 2006], namely Observatoire de Haute-Provence (OHP) in France (43.93^{o}N, 5.71^{o}E), Mauna Loa, Hawaii (19.5^{o}N, 155.7^{o}W), and the Table Mountain Facility, California (34.5^{o}N, 117.7^{o}W). These lidars are high power differential absorption lidars (or DIAL) which make precise measurements of stratospheric ozone concentration profiles from ~20 to 50 km altitude. This technique requires two (or more) laser wavelengths which are chosen such that one coincides with a region of high absorption, specific to the species being measured, and the other is tuned into the wings of this feature to a wavelength with much lower absorption. The concentration of ozone is retrieved by measuring the different absorption of the backscatter data at the two wavelengths.

The estimated accuracy (or systematic uncertainty) for the Table Mountain Facility ozone number density lidar profiles is below 0.05×10^{18} molecules/m^3 (or 1-5%) for the vertical range 15-50 km and can occasionally increase to 0.3×10^{18} molecules/m^3 (or 10-50%) for heights below 15 km. The translation to mixing ratio adds another 1-3% uncertainty due to the use (and associated uncertainty) of external measurements or model outputs of pressure and temperature. The temperature and pressure data used for OHP correspond to nearby radiosoundings performed daily in Nimes, complemented at higher altitude by the CIRA [CIRA1986] model. Hawaii and Table Mountain lidars use NCEP operational analysis data interpolated to the location and time of the lidar measurements, and local Hilo radiosondes complement the Hawaii database.

Figure 13 shows the averaged profiles of available MLS v2.2 data and coincident lidar measurements and their differences at the three lidar stations. The comparisons with the troposheric ozone lidar measurements at Table Mountain Facility are discussed later. MLS v2.2 shows better agreements with lidar data than v1.5. MLS v2.2 ozone gives best agreement with lidar in the 2 hPa to 50 hPa region where the differences are about 5%. The relatively larger differences around 1 hPa for all three stations may be caused by day/night MLS ozone differences or poorer lidar measurements in this region. For the Haute Provence station, averaged differences are about 5% at 100 and 146 hPa, and 20% at 215 hPa. At 147 hPa, MLS v2.2 ozone is lower by ~20% (uncertainty 10%) compared to both the Mauna Loa and the Table Mountain Facility measurements. On average, based on these three stations, MLS v2.2 agrees with lidar measurements to better than ~5% down to 100 hPa. The comparisons also show larger standard deviations of the mean difference for pressures of 100 hPa and larger.

MLS low altitude ozone shows good agreement with that measured by the Table Mountain tropospheric ozone lidar, shown in Figure 14. This measurement system provides a more reliable comparison for altitude region. The differences between MLS v2.2 ozone and lidar are within 3% in the lower stratosphere and within 8% at the largest pressures. The estimated precisions are within 10% at pressure levels less than 100 hPa and increase to 25% for pressures larger than 100 hPa. The standard deviations of the mean differences (dashed lines) are higher than 10% and increase to more than 50% in the upper troposphere. This analysis indicates that the MLS ozone in the UT/LS agrees with the Table Mountain tropospheric ozone lidar measurements with no significant biases. Figure 14 also highlights the better agreement versus lidars for MLS v2.2 than MLS v1.5 data. The calculations of partial column ozone abundances over the three lidar stations indicate that MLS v2.2 data agree with the lidars to better than 5%. In Figure 15, we present the time series of MLS ozone, ozonesonde measurements at Boulder, Colorado and lidar measurements at Table Mountain Facility in 2004, 2005 and 2006 at three pressure levels. These two stations are the closest stations we can find for the comparisons of the three different kinds of measurements, and they should have similar spatial and temporal ozone variability. In general, the MLS v2.2 ozone tracks both the ozonesonde and lidar measurements well as a function of season. The ozone abundance at 215 hPa shows a weak seasonal variability with enhanced values around spring, but shows a strong seasonal cycle at both 46 and 10 hPa. The ozone distribution reaches its maximum in the summer at 10 hPa, while it reaches its maximum in the spring at 46 hPa.

5. Summary and Conclusions

This paper presents the validation results of newly-released Aura MLS v2.2 ozone in the upper troposphere and lower stratosphere using worldwide ozonesonde and ground-based lidar measurements. In the upper troposphere and lower stratosphere, MLS ozone is generally biased high at mid- to high latitudes, as compared to ozonesondes, but within 20% or 20 ppbv, on average, in the tropics. In the middle stratosphere, MLS is within 7% of the global ozonesonde measurements. Averaged over each ozonesonde station, the column ozone comparisons against MLS show better than 10% agreement, but there is no significant bias globally.

Comparisons to three sets of lidar measurements from Hawaii, Table Mountain, and Haute Provence in France show excellent agreement (within about 5%) in the stratosphere and 8% down to 215 hPa. This study also shows that the temporal variations in MLS ozone and in midlatitude ozone from the Boulder, CO, ozonesondes and the Table Mountain Facility, CA, lidar track each other very well. The global results of comparisons between ozonesondes and lidars are listed in Tables 3 and 4. The results from the lidar comparisons show better agreement with the MLS data in the lower altitude range in particular. This may indicate, in part, added variability (and resulting biases) in comparisons with a large number of sites using different sondes, and possibly a bias between the lidars and sondes. However, the comparisons between MLS ozone and aircraft in situ and lidar data do not give strong evidence for a high MLS bias at 215 hPa of more than 15% [*Livesey et al*., 2007; *Froidevaux et al*., 2007]. Because of the somewhat inconsistent evidence of a high MLS bias at 215 hPa, the accuracy estimate for MLS v2.2 ozone at 215 hPa has been set at about 20 ppbv + 20% (see the above references), rather than the somewhat lower estimate of 20 ppbv + 10% expected from

simulations and sensitivity studies (see the above two references). Further detailed investigations using more reprocessed MLS v2.2 data may shed more light on these issues.

Table 3. Summary of comparisons between MLS ozone and ozonesonde data (global).

Pressure (hPa)	Difference with Sonde (%)	Combined Precision (%)	Standard Deviation of Differences (%)
215.4	25	20	87
146.8	0	10	30
100.0	2	6	28
< 100 and >5	5	6	18

Table 4. Summary of comparisons between MLS ozone and lidar data (3 sites).

Pressure (hPa)	Difference with Lidar (%)	Combined Precision (%)	Standard Deviation of Differences (%)
215.4	8	25	80
146.8	-4	15	32
100.0	2	12	40
< 100 and >5	5	10	20

Acknowledgements

This work at the Jet Propulsion Laboratory, California Institute of Technology, was performed under contract with the National Aeronautics and Space Administration. We are very grateful to the MLS instrument and data/computer operations and development team (at JPL and from Raytheon, Pasadena) for their support through all the phases of the MLS project, in particular D. Flower, G. Lau, J. Holden, R. Lay, M. Loo, G. Melgar, D. Miller, B. Mills, M. Echeverri, E. Greene, A. Hanzel, A. Mousessian, S. Neely, C. Vuu, and P. Zimdars. We greatly appreciate the work of those involved in the Aura Validation Data Center at the NASA Goddard Space Flight Center, as this has been the main data repository for Aura correlative/validation data since the Aura launch. Thanks to Jennifer Logan for providing the WOUDC data. Thanks to the Aura Project for their support throughout the years (before and after the Aura launch), in particular M. Schoeberl, A. Douglass (also as co-chair of the Aura validation working group), E. Hilsenrath, and J. Joiner. We also acknowledge the support from NASA Headquarters, P. DeCola for MLS and Aura, and M. Kurylo, J. Gleason, B. Doddridge, and H. Maring, especially in relation to the Aura validation activities and campaign planning efforts.

References

Bodeker, G.E., I.S. Boyd, and W.A. Matthews, Trends and variability in vertical ozone and temperature profiles measured by ozonesondes at Lauder, New Zealand: 1986-1996, *J. Geoph. Res*., 103 (D22), 28661-28681, 1998.

Borchi, F., J.-P. Pommereau, A. Garnier, and M. Pinharanda (2005), Evaluation of SHADOZ sondes, HALOE and SAGE II ozone profiles at the tropics from SAOZ UV-Vis remote measurements onboard long duration balloons, *Atmos. Chem. Phys.*, 5, 1381-1397.

De Muer *et al.*, Comparison of SageII ozone measurements and ozone soundings at Uccle during the periods Feb 1985 - Jan 1986, *J. Geoph. Res*., 95, 11903-11911, 1990.

Froidevaux, L., *et al.* (2006), Early validation analyses of atmospheric profiles from EOS MLS on the Aura satellite, *IEEE Transactions on Geoscience and Remote Sensing*, 44, NO. 5, 1106-1121.

Froidevaux, L., *et al.* (2007), Validation of Aura Microwave Limb Sounder Stratospheric ozone measurements, *J. Geophys. Res.*, submitted to the Aura validation special issue.

Godin S., G. Mgie, J. Pelon : Systematic Lidar Measurements of the Stratospheric Ozone vertical Distribution, Geophys. Res. Letters, Vol 16 No 16, 547-550, 1989.

Godin-Beekmann, S., J. Porteneuve, A. Garnier, Systematic DIAL ozone measurements at Observatoire de Haute-Provence, *J. Env. Monitoring*, 5, 57-67, 2003.

Hocke, K., N. Kampfer, D. G. Feist, H. Calisesi, J. H. Jiang, and S. Chabrillat (2006), Temporal Variance of Lower Mesospheric Ozone Over Switzerland During Winter 2000/2001, *Geophys. Res. Lett.*, 33, L09801, doi:10.1029/2005GL025496.

Jourdain, L., *et al.* (2007), Tropospheric vertical distribution of tropical Atlantic ozone observed by TES during the Northern African biomass burning season, *Geophys. Res.* Lett., 34, L04810, doi:10.1029/2006GL028284.

Kar, J., C. R. Trepte, L. W. Thomason, J. M. Zawodny, D. M. Cunnold, and H. J. Wang (2002), On the tropospheric measurements of ozone by the Stratospheric Aerosol and Gas Experiment II (SAGE II, version 6.1) in the tropics, *Geophys. Res. Lett.*, 29, NO. 24, 2208, doi:10.1029/2002GL016241.

Kerr, J.B., H. Fast, C.T. McElroy, S.J. Oltmans, J.A. Lathrop, E. Kyro, A. Paukkunen, H. Claude, U. Khler, C.R. Sreedharan, T. Takao and Y. Tsukagoshi (1994), The 1991 WMO international ozonesonde intercomparison at Vanscoy, Canada,. *Atmosphere-Ocean*, 32, 685-716.

Leblanc, T., and McDermid, I. S. (2000), Stratospheric ozone climatology from Lidar measurements at Table Mountain (34.4 degrees N, 117.7 degrees W) and Mauna Loa (19.5 degrees N, 155.6 degrees W), *J. Geophys. Res.*, 105, 14613-14623.

Leblanc, T., *et al.*, Simultaneous lidar and EOS MLS measurements, and modeling, of a rare polar ozone filament event over Mauna Loa Observatory, Hawaii, *Geophys. Res. Lett.*, 33 (16): Art. No. L16801, 2006

Livesey, N. J., *et al.* (2005), EOS MLS version 1.5 Level 2 data quality and description document, *Tech. rep.*, Jet Propulsion Laboratory, D-32381.

Livesey, N. J., *et al.* (2007), Validation of Aura Microwave Limb Sounder O3 and CO observations in the upper troposphere and lower stratosphere, *J. Geophys. Res.*, to be submitted to the Aura validation special issue.

McDermid, I. S., Godin, S. M., and Walsh T. D. (1991), Lidar measurements of stratospheric ozone and intercomparisons and validation, *Applied Optics*, 29.

Read, W.G., Z. Shippony, M.J. Schwartz, N.J. Livesey, and W.V. Snyder (2006), "The clear-sky unpolarized forward model for the EOS Microwave Limb Sounder (MLS)," IEEE *Trans. Geosci. Remote Sensing,* 44, no. 5, 1367-1379.

CIRA1986, D. Rees (ed.), Advances in Space Research, Volume 8, Number 5-6, 1988.

Rodgers, C. D. (1976), Retrieval of atmospheric temperature and composition from remote measurements of thermal radiation, *Reviews of Geophysics and Space Sciences,* 14, 609 - 624.

Schwartz, M.J., et al. (2007), Validation of Aura Microwave Limb Sounder temperature and geopotential height measurements, *J. Geophys. Res.*, this issue, submitted.

Sauvage, B., V. Thouret, A. M. Thompson, J. C. Witte, J.-P. Cammas, P. Nedelec, and G. Athier (2006), Enhanced view of the “tropical Atlantic ozone paradox” and “zonal wave one” from the in situ MOZAIC and SHADOZ data, *J. Geophys. Res.*, 111, D01301, doi:10.1029/2005JD006241.

Schoeberl, M. R., *et al*. (2004), Earth Observing System missions benefit atmospheric research, Experiment, *Trans. EOS, AGU*, 85, NO. 18, 177-181.

Schoeberl, M. R., *et al*. (2006), Overview of the EOS Aura mission, Experiment, *IEEE Transactions on Geoscience and Remote Sensing*, 44, NO. 5, 1066-1074.

Smit, H. G. J., W. Straeter, B. Johnson, S. Oltmans, J. Davies, D. W. Tarasick, B. Hoegger, R. Stubi, F. Schmidlin, T. Northam, A. Thompson, J. Witte, I. Boyd and F. Posny (2007), Assessment of the performance of ECC-ozonesondes under quasi-

flight conditions in the environmental simulation chamber: Insights from the Jlich Ozone Sonde Intercomparison Experiment (JOSIE), *J. Geophys. Res.*, in press.

Sparling, L. C., J. C. Wei, and L M. Avallone (2006), Estimating the impact of small-scale variability in satellite measurement validation, *J. Geophys. Res.*, 111, D20310, doi:10.1029/2005JD006943.

Thompson, A. M., *et al*. (2003), Southern hemisphere additional ozonesondes (SHADOZ) 1998-2000 tropical ozone climatology 2. Tropospheric variability and the zonal wave-one, *J. Geophys. Res.*, 108, NO. D2, 8241, doi:10.1029/2002JD002241.

Thompson, A. M., J. C. Witte, H.G. Smit, S.J Oltmans, B.J. Johnson, V.W.J.H. Kirchhoff and F.J. Schmidlin (2007), Southern Hemisphere Additional Ozonesondes (SHADOZ) 1998\u20132004 tropical ozone climatology: 3. Instrumentation, station-to-station variability, and evaluation with simulated flight profiles, *J. Geophys. Res.* 2005JD007042, in press.

Waters, J. W. (2000), An overview of the EOS MLS Experiment, JPL, Pasadena, CA, Tech. Rep. JPL D-15745, 1.1 ed..

Waters, J. W., *et al*. (2006), The Earth Observing System Microwave Limb Sounder (EOS MLS) on the Aura satellite, Experiment, *IEEE Transactions on Geoscience and Remote Sensing*, 44, NO. 5, 1075-1092.

World Climate Research Programme (1998), SPARC/IOC/GAW Assessment of Trends in the Vertical Distribution of Ozone, Stratospheric Processes and Their Role in Climate, World Meteorol. Organ. Global Ozone Res. Monit. Proj. Rep. 43, Geneva, Switzerland.

Yang, D., D. M. Cunnold, H.-J. Wang, and L. Froidevaux (2007), Mid-latitude tropospheric ozone columns derived from Aura OMI and MLS data using the TOR approach and mapping techniques, *J. Geophys. Res.*, submitted.

Ziemke, J. R., S. Chandra, B. N. Duncan, L. Froidevaux, P. K. Bhartia, P. F. Levelt, J. W. Waters (2006), Tropospheric ozone determined from Aura OMI and MLS: Evaluation of measurements and comparison with the Global Modeling Initiative's Chemical Transport Model, *J. Geophys. Res.*, 111, D19303, doi:10.1029/2006JD007089.

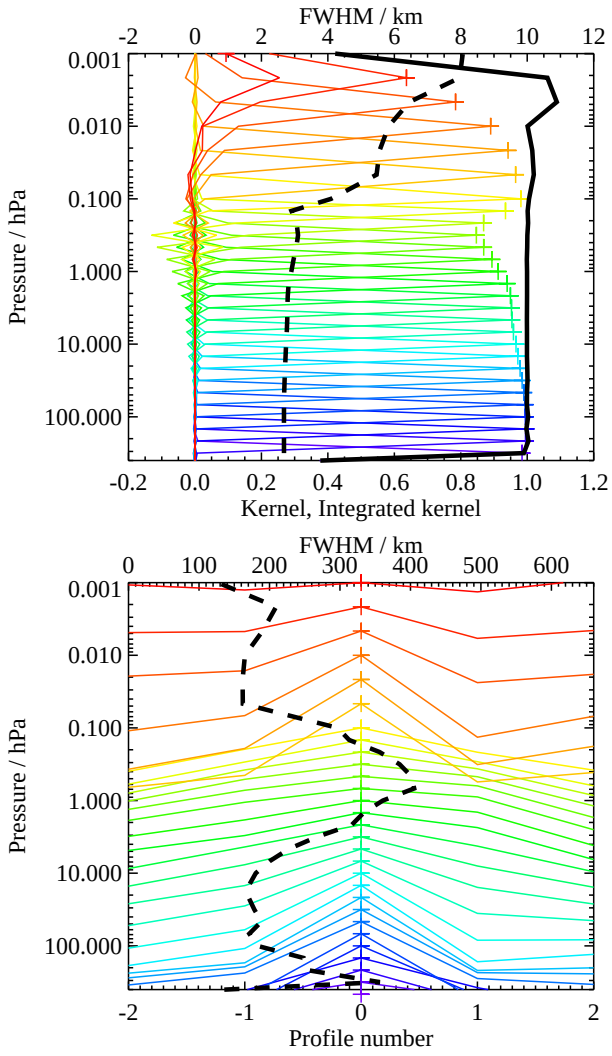

Figure 1. Representative averaging kernels (colored lines) and resolution for the v2.2 MLS standard ozone product (from 240 GHz radiances). This example is for 35° N and results for other latitudes are very similar. Top panel: Colored lines show the vertical averaging kernels as a function of the MLS retrieval level, indicating the region of the atmosphere from which information is contributing to the measurements on the individual retrieval surfaces, which are denoted by the plus signs. The kernels are integrated in the horizontal dimension for 5 along-track scans. The dashed black line is the full width at half maximum (FWHM) of these averaging kernels, and indicates the vertical resolution, as given in kilometers above the top axis. The solid black line shows the integrated area under each of the colored curves; a value near unity indicates that most of the information at that level was contributed by the measurements, whereas a lower value implies significant contribution from a priori information. Bottom panel: Colored lines show the horizontal averaging kernels (integrated in the vertical dimension) and dashed black line gives the horizontal resolution, from the FWHM of these averaging kernels (top axis, in km). The averaging kernels are scaled such that a unit change is equivalent to one decade in pressure. Profile numbers along the MLS orbit track are given on bottom axis, with negative values referring to the satellite side of the atmosphere, with respect to the tangent point profile (profile zero); profiles are spaced every 1.5°great circle angle, or about 165 km, along the orbit track.

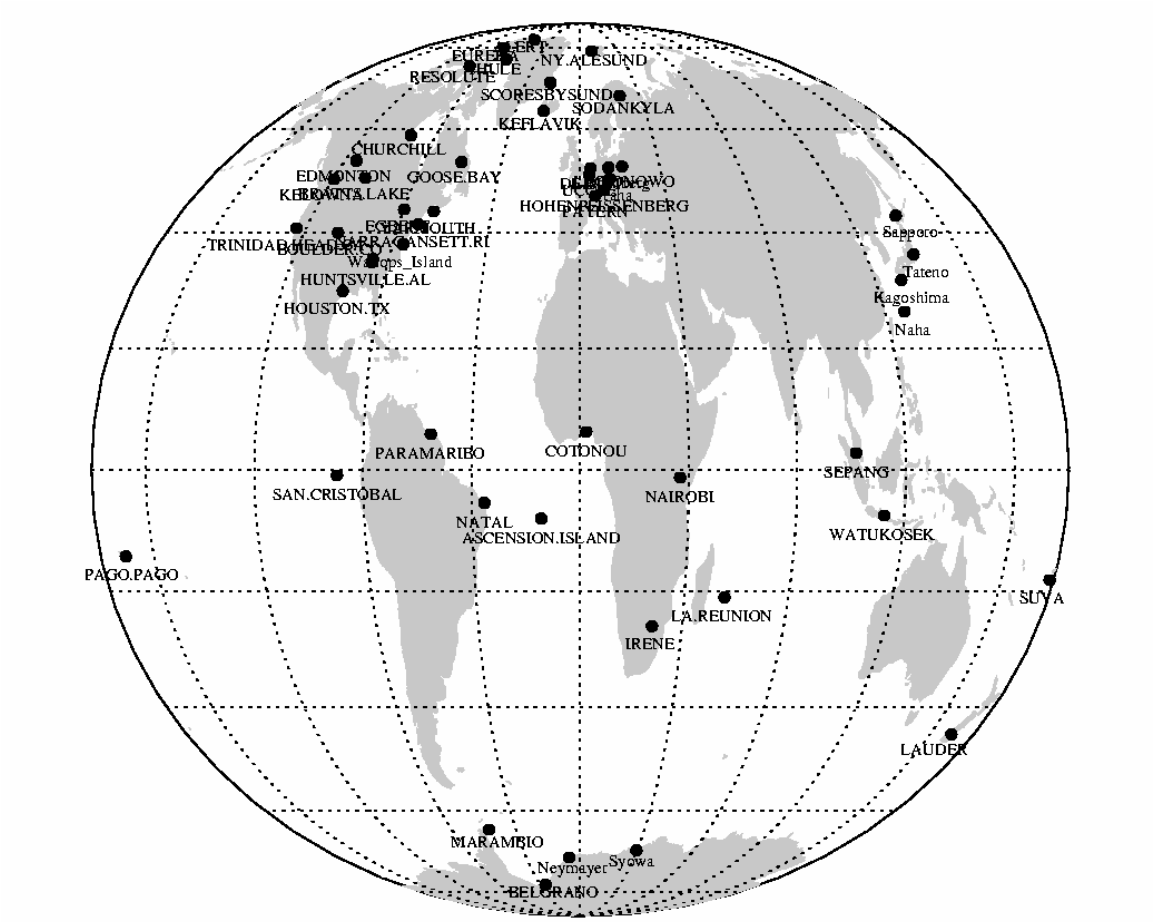

1
2 Figure 2. Global distribution of ozonesonde stations considered in this work.

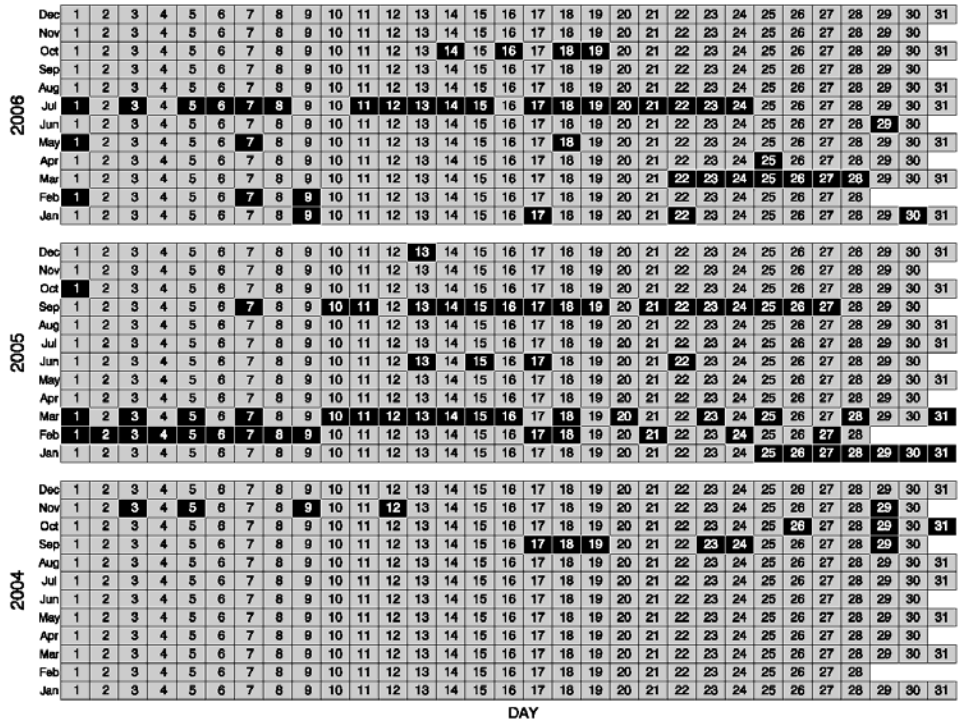

Figure 3. Days (black square) when coincident ozone profiles were found in 2004, 2005 and 2006 between available MLS version 2.2 and ozonesonde measurements.

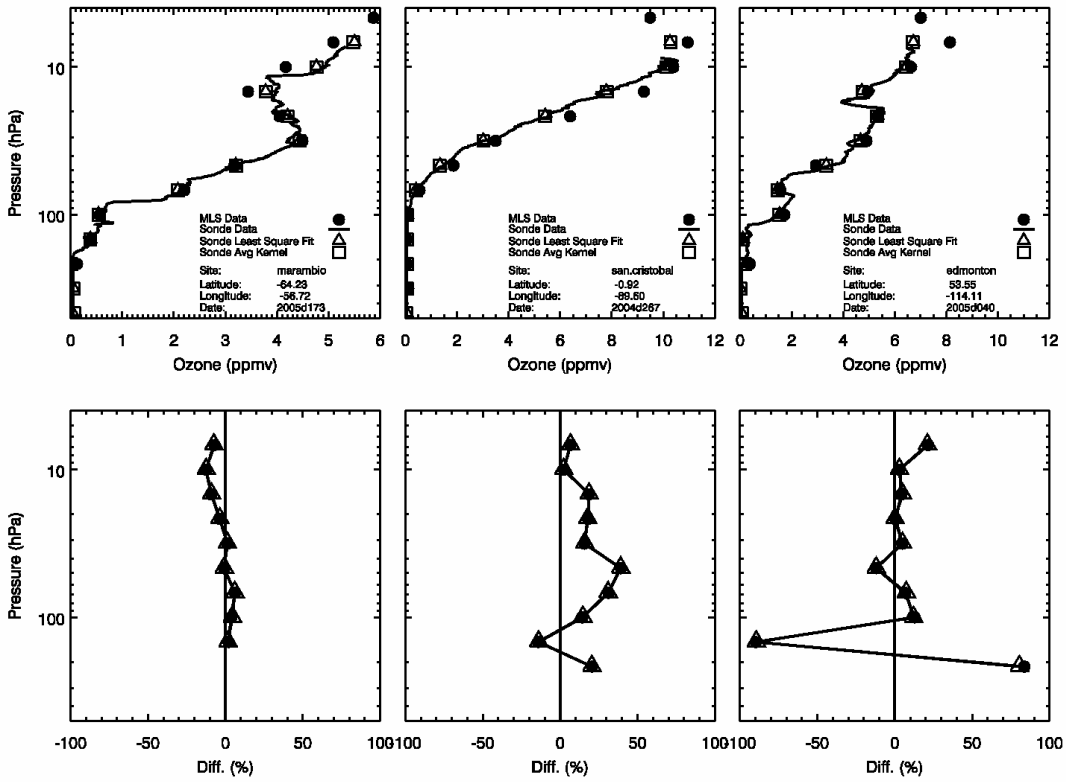

Figure 4. Selected ozonesonde profiles and their translation to the MLS pressure grid by using least squares fit or averaging kernel methods in the southern high latitudes (left panel), equatorial region (center panel), and northern high latitudes (right panel). In the top panel, the black line gives the ozonesonde high resolution profile, the dots are the MLS data, open squares are the ozonesonde data smoothed by the averaging kernels (see text), and open triangles are the ozonesonde data smoothed by a least squares fit. The bottom panel shows the percentage differences between MLS and ozonesonde data, dots give results using MLS averaging kernels, and open triangles are results from the least squares fit.

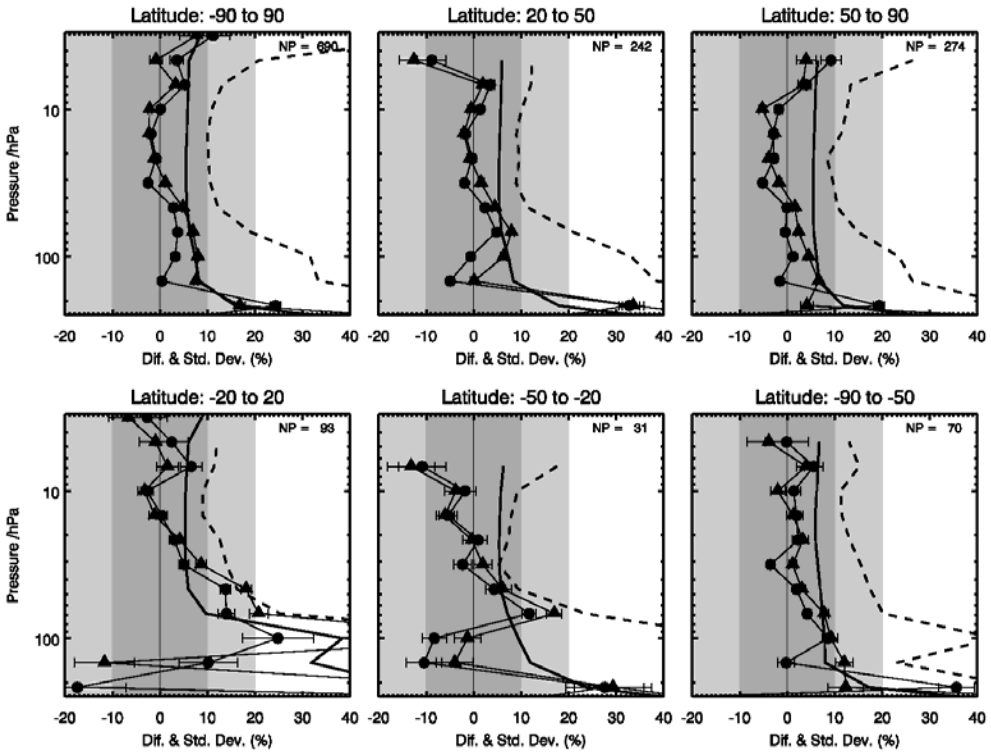

Figure 5. Comparisons between MLS v2.2, v1.5 ozone and ozonesonde measurements in 6 latitude bins. Filled circle and connected line represents the averaged percentage differences between v2.2 and ozonesondes, while filled triangle and connected line shows the averaged percentage differences between v1.5 and ozonesondes. Dashed line gives the standard deviation of the differences (in percent) between v2.2 and ozonesondes. Heavy solid line shows the combined precisions (in percent) for v2.2 and ozonesondes, using 5% precision for the sondes. The error bar on each data point (dot) is twice the precision in the mean differences (and is often too small to see).

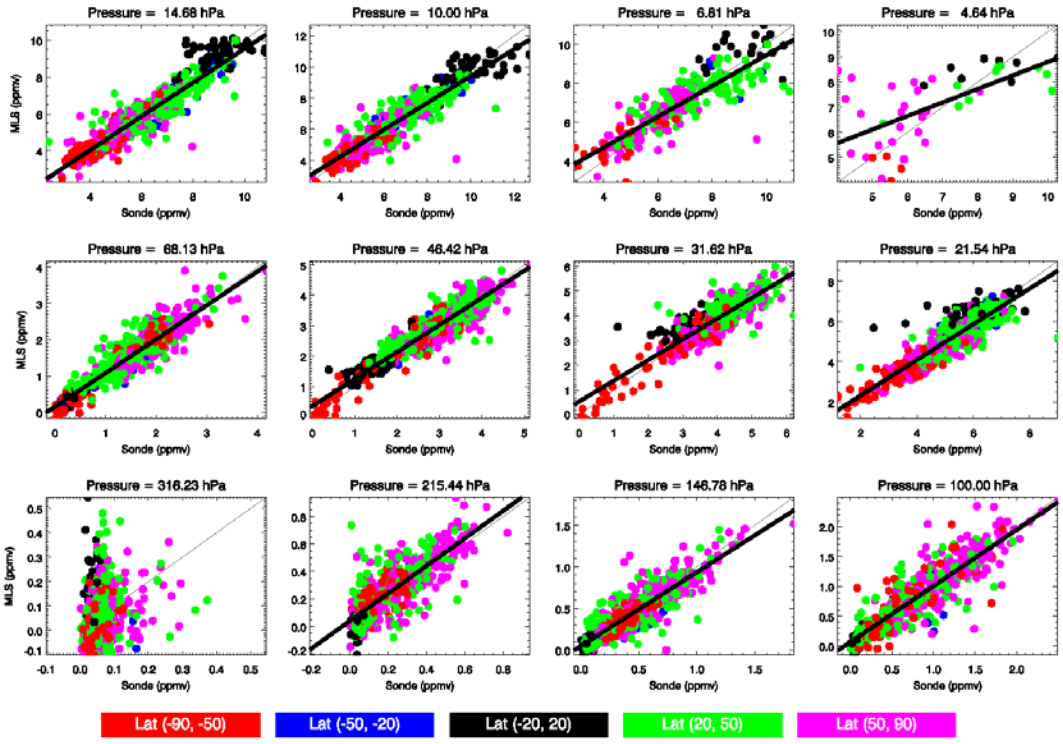

Figure 6. Scatter plots of MLS versus ozonesondes from all the stations for all the coincidences on selected pressure levels, color-coded in 5 latitude bins. The heavy black lines are the linear fits to the data.

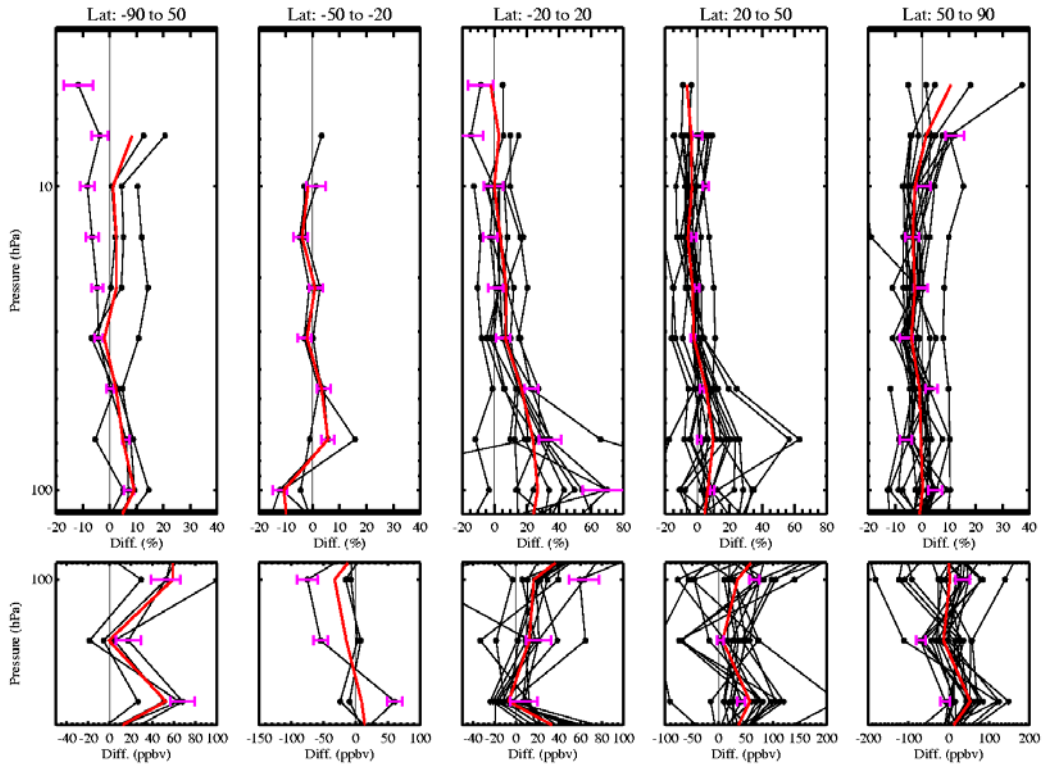

Figure 7. Averaged ozone profiles differences between MLS v2.2 and ozonesondes for each station, in 5 latitude bins. The top panel shows the profiles at pressure 120-3 hPa, and the bottom panel at pressure 250-80 hPa. The red lines are the averaged profiles. Note that the differences are given in ppbv for the upper troposphere/lower stratosphere region (bottom panel) and as a percentage for the stratosphere (top panel). The error bars (pink) are examples of the 2σ combined precisions for sites Syowa, Lauder, Hawaii, Hohenpeissenberg and De Bilt, in their respective latitude bins. Precisions in the averages for each bin (red curves) are even smaller (and are not shown).

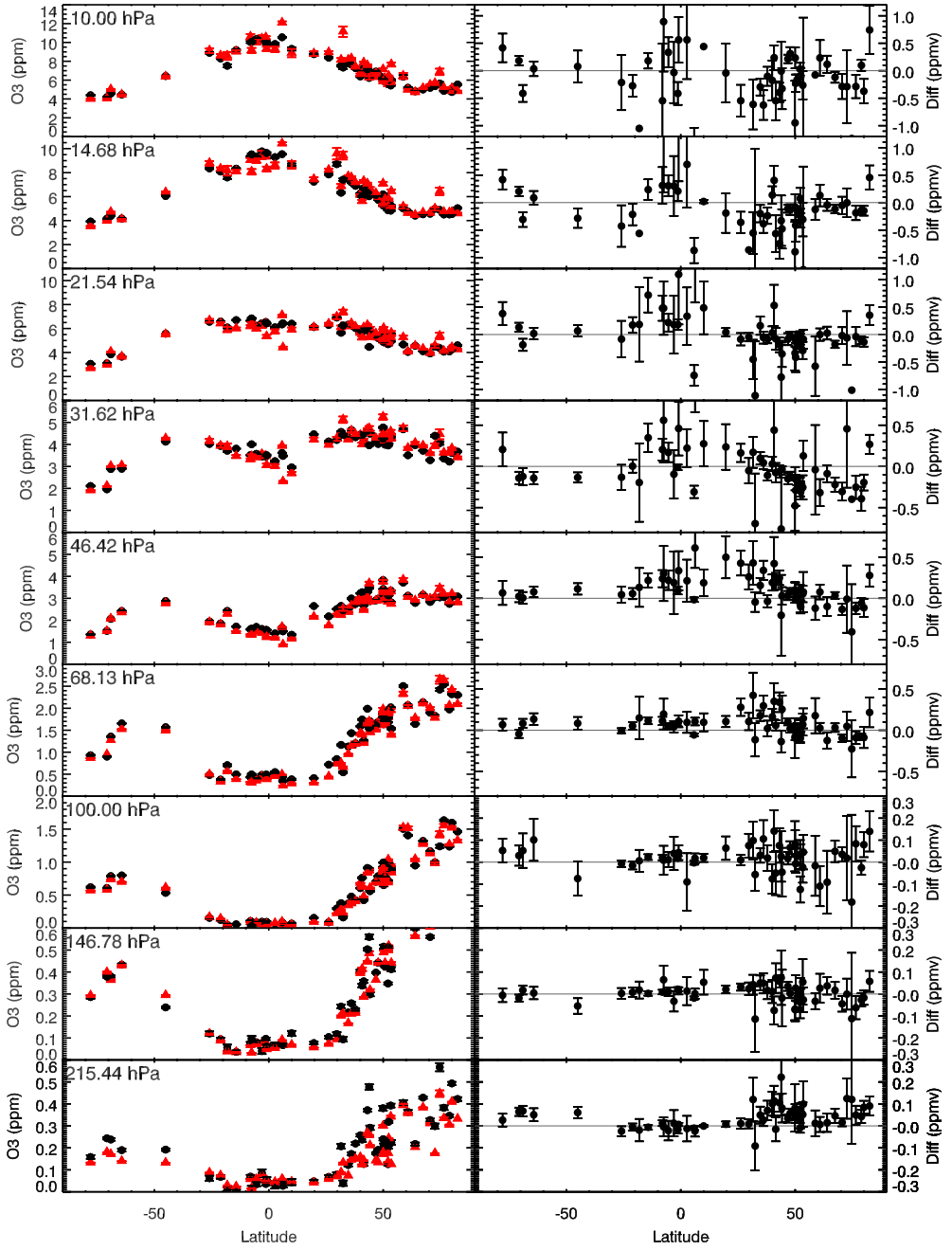

Figure 8. Left panels: Latitudinal distributions of average ozone from each ozonesonde station (red triangles) compared with MLS ozone data (black dots) on selected pressure levels, as indicated. The error bars are the standard deviation (variability). Right panels: Differences (MLS minus sonde data) in ppmv. The error bars show twice the standard error in the mean differences.

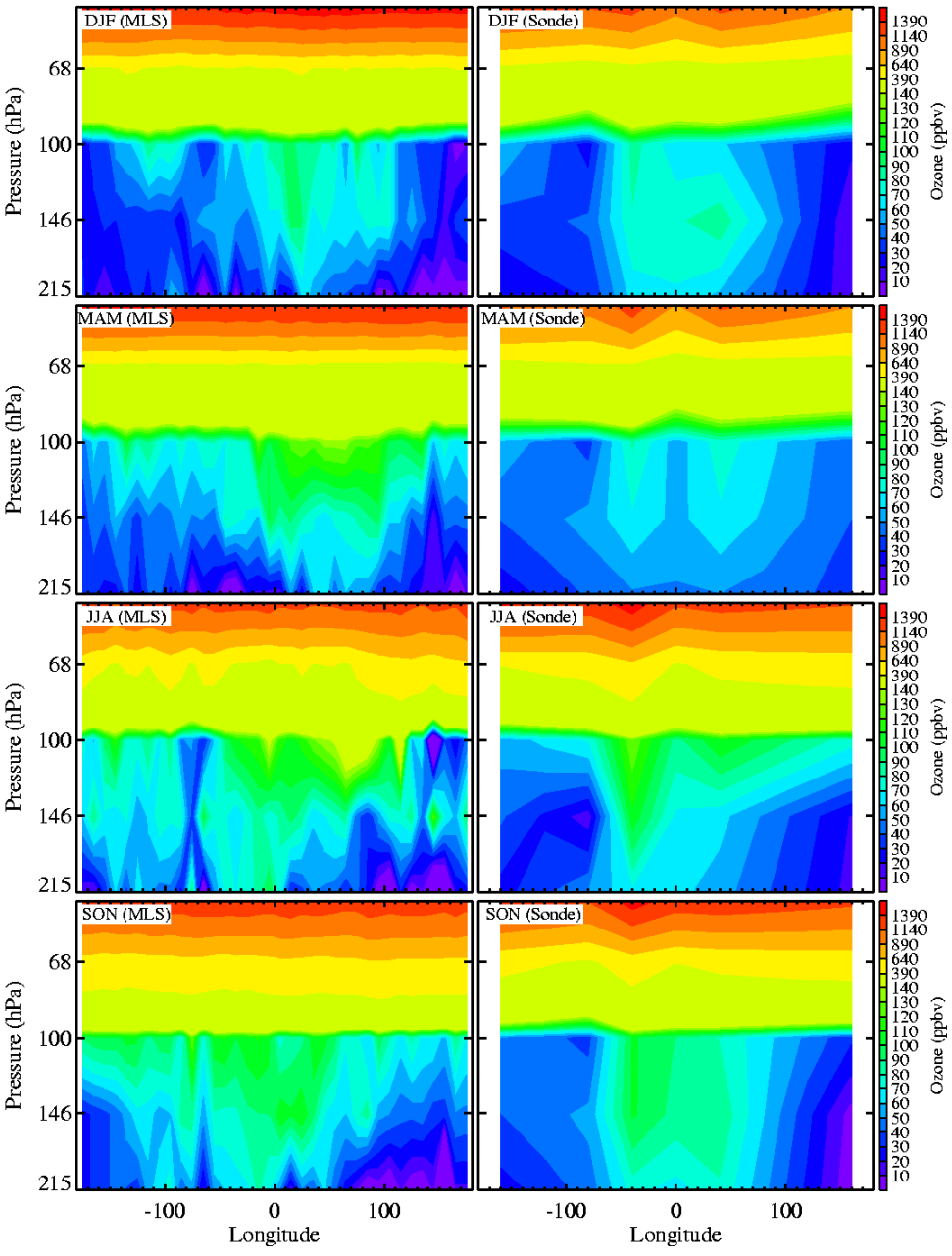

Figure 9. Ozone vertical distribution from 20 hPa to 215 hPa in the equatorial region for four seasons (months indicated by first letters at top left for each panel), using 2004 and 2005 data. The left panel is from the MLS v1.5 ozone data and the right panel is from the ozonesonde measurements, which mostly come from the SHADOZ network.

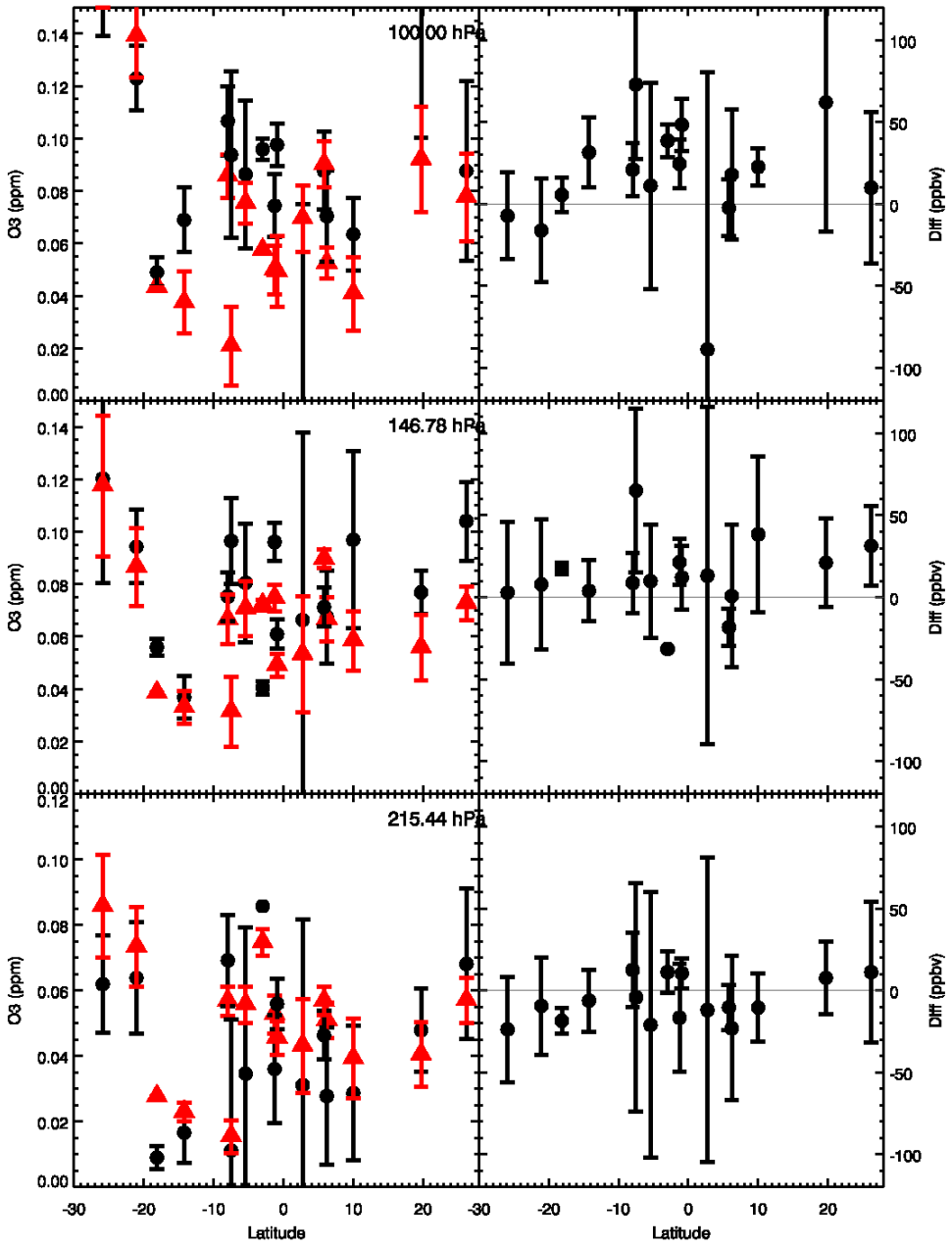

Figure 10. Latitudinal distributions of averaged ozone at each low latitude ozonesonde station (red triangles), with the standard deviation (variability) shown as error bars (red bar), compared with MLS ozone data (black dots) and their error bars (black bar) at three pressure levels (left panel). The right panel shows the differences (MLS minus ozonesonde data) in ppbv. The error bars show twice the standard error in the mean differences.

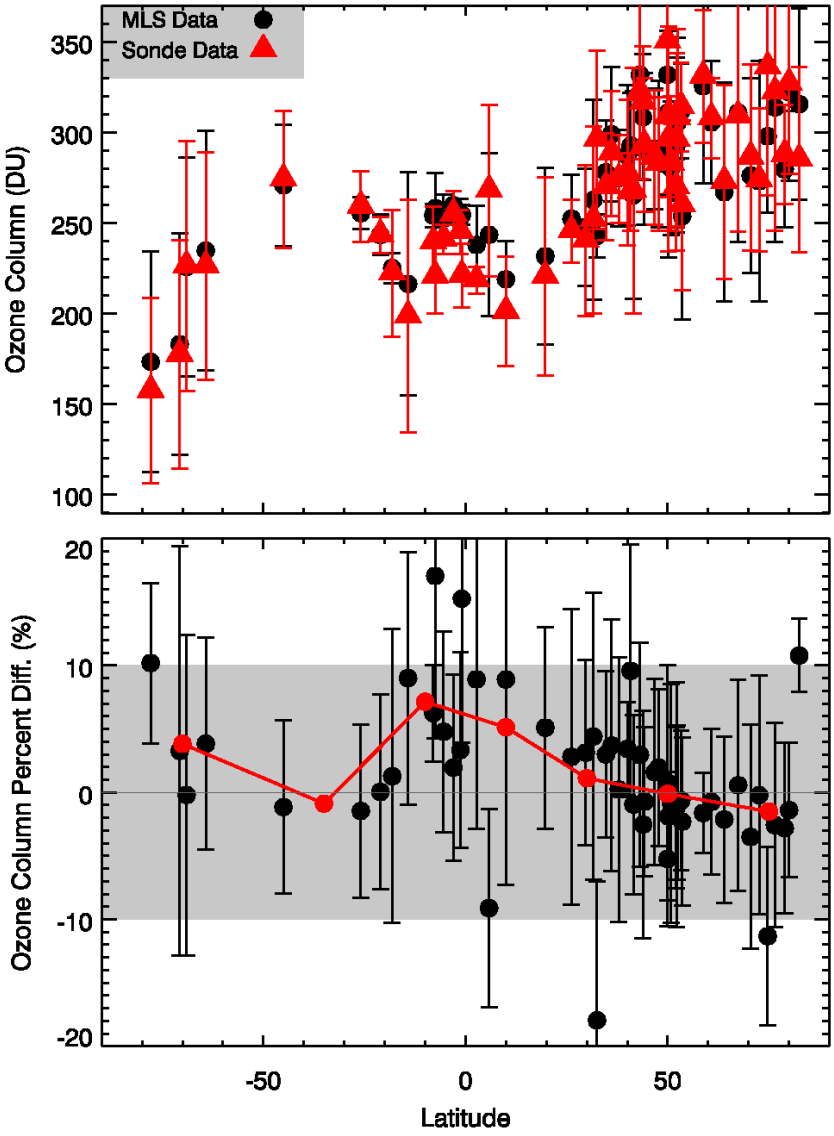

Figure 11. Averaged column ozone in each station as compared with MLS ozone data (top panel), and their differences in percentage (bottom panel). In the top panel, the black circles are the MLS column ozone with the standard deviation (variability) and ozonesonde columns are represented by red triangles with the standard deviation (variability). The bottom panel shows column differences between MLS ozone and ozonesondes with twice the standard error in the mean differences. The (connected) red dots represent the averaged differences over 20^{o} latitude bins in the northern hemisphere and 30^{o} latitude bins in the southern hemisphere.

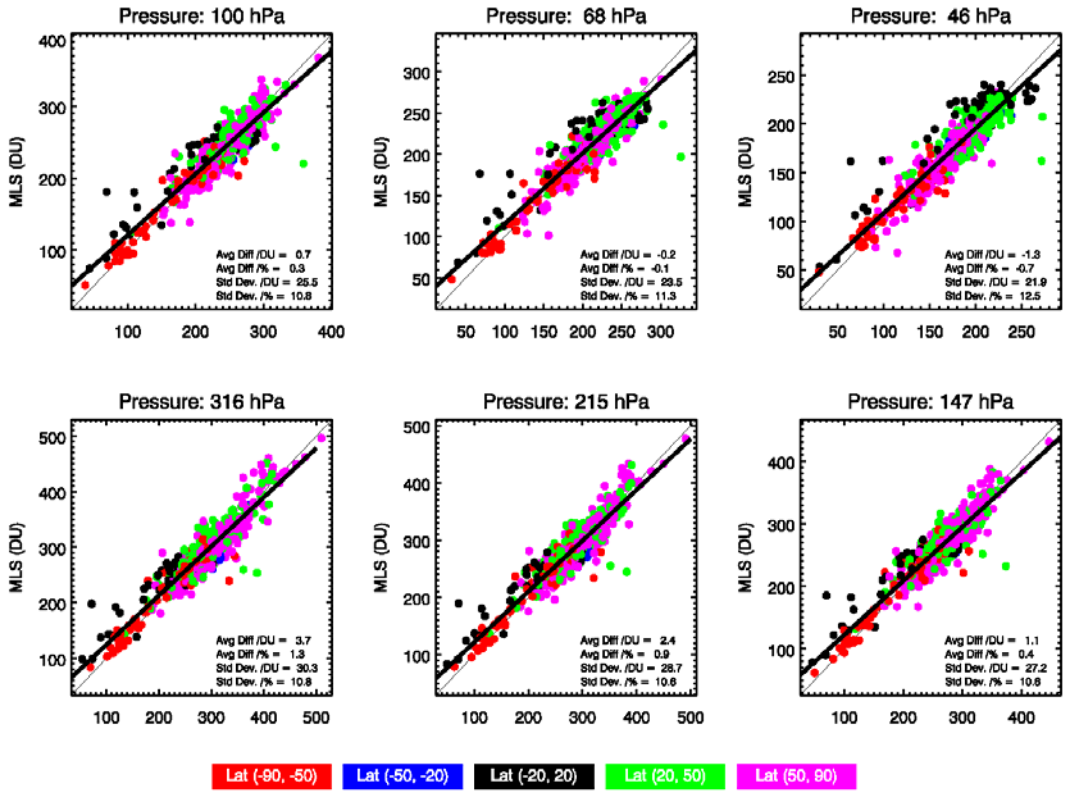

Figure 12. Scatter plots of MLS ozone columns versus ozonesonde columns above six selected pressure levels from all the stations for all the coincidences, color-coded in 5 latitude bins. The heavy black lines are the linear fits to the data.

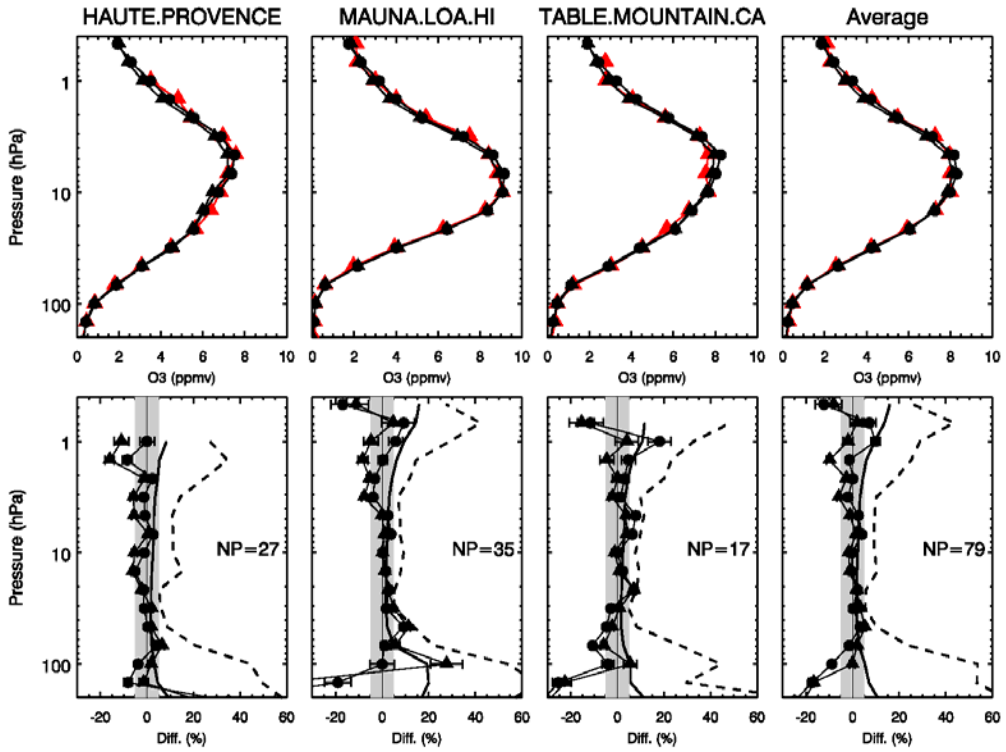

Figure 13. Comparisons between MLS v2.2, v1.5 ozone and lidar measurements at three stations. The averaged profiles of MLS v2.2 (filled circle), v1.5 (filled triangle) and lidar (red filled triangle) are shown in the top row. In the second row, the filled circles represent the average percentage differences between MLS v2.2 and lidar data, while the filled triangles show the average percentage differences between MLS v1.5 and lidar data. Error bars represent twice the precision (standard error) in these mean differences. Dashed lines give the standard deviations of the mean differences between v2.2 and lidar data. Heavy solid line shows the combined precisions for the v2.2 and lidar measurements. The shaded area is the ±5% region.

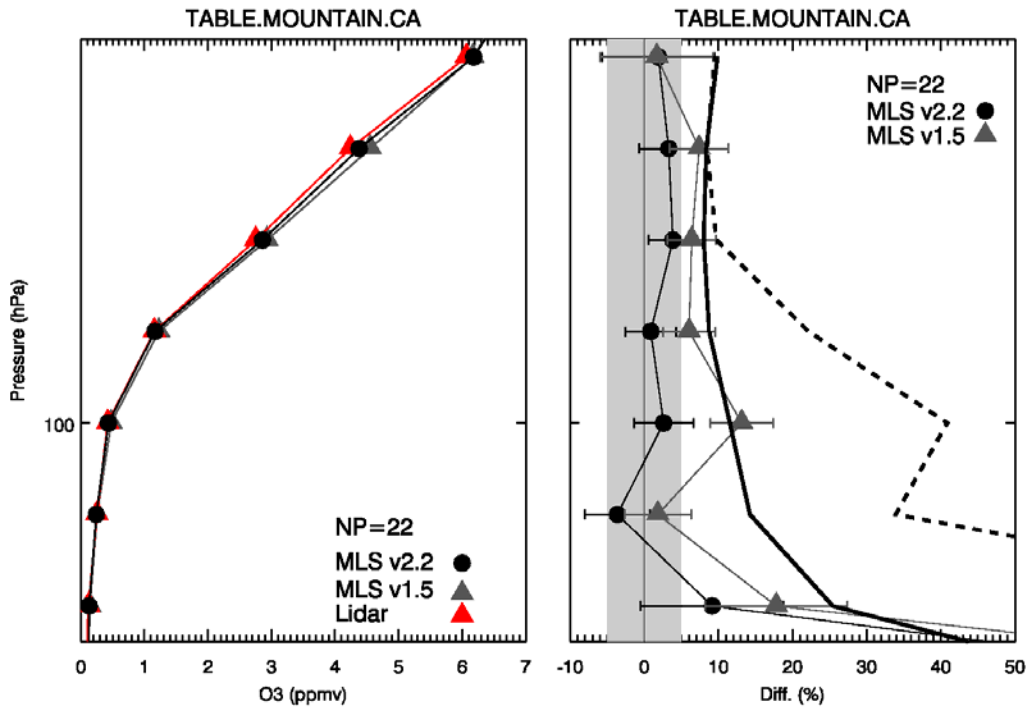

Figure 14. Same as Figure 13 except that the lidar data are from the Table Mountain Facility tropospheric ozone measurements; and the pressure levels are from 215 to 22 hPa.

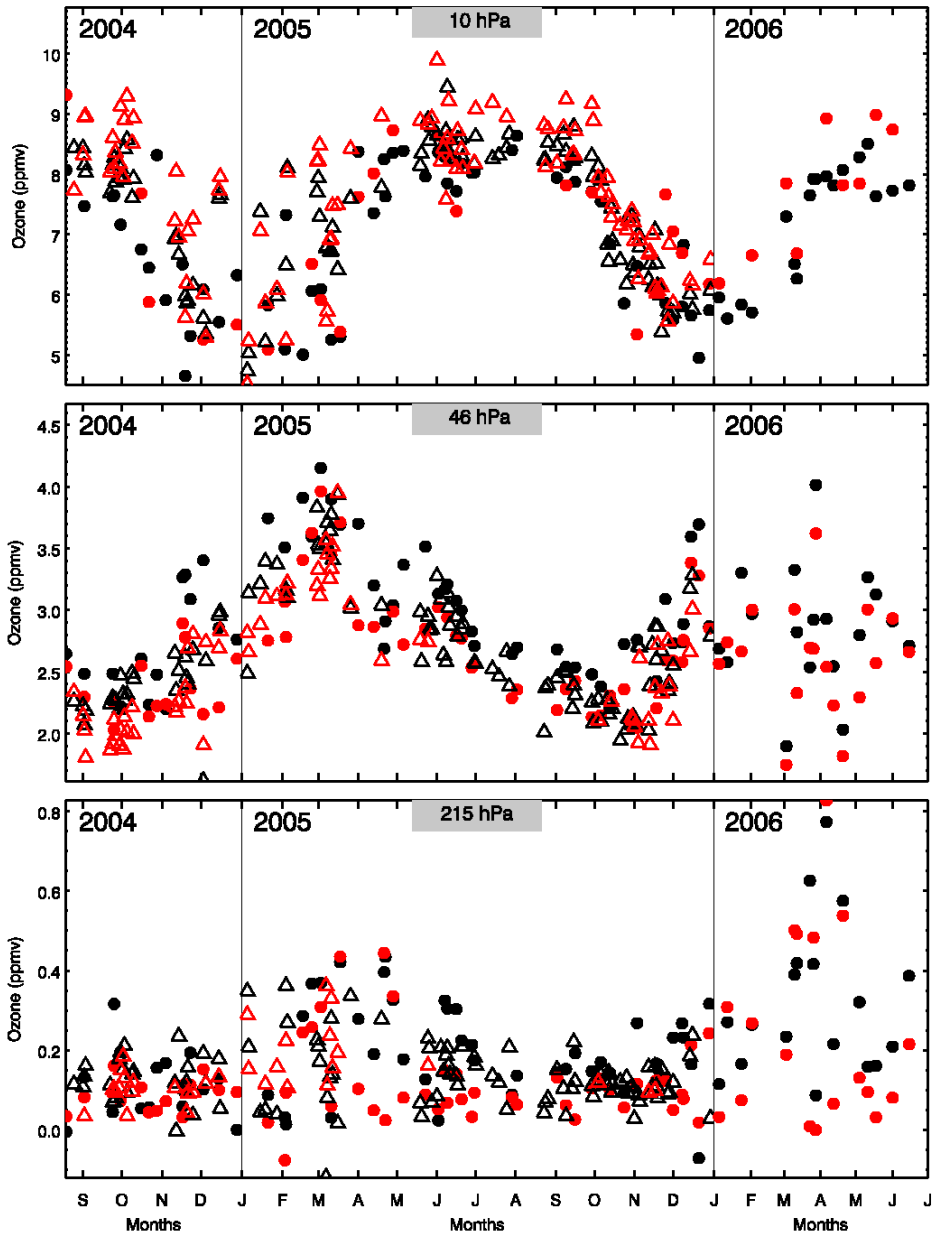

Figure 15. Time series comparisons between MLS v2.2 ozone (black open triangle) and lidar (red open triangle) measurements at Table Mountain, and between MLS v2.2 ozone (black dot) and ozonesonde (red dot) measurements at Boulder, Colorado in 2004, 2005 and 2006 at three selected pressure levels (10, 46, 215 hPa).